



Hydrolysis of Congo red in subcritical water in the presence of CeO₂/ZSM5 catalyst

Xu Zhang^a, Fan Yang^a, Jialing Qin^b, Huanghu Peng^a, Zezhou Chen^a, Lei Che^a, Shouxin Zhu^a, Wei Yang^{a,b,*}

^aCollege of Engineering, Huzhou University, No. 759, East 2nd Road, Huzhou 313000, China, Tel. +86-572-232-0692; emails: wei_yang15@hotmail.com (W. Tang), zhangxu@zjhu.edu.cn (X. Zhang), 02567@zjhu.edu.cn (F. Yang), penghh@zjhu.edu.cn (H.H. Peng), 02643@zjhu.edu.cn (Z.Z. Chen), three_stone_cn@163.com (L. Che), zsx@zjhu.edu.cn (S.X. Zhu)

^bCollege of Materials and Environmental Engineering, Hangzhou Dianzi University, Xiasha University Park, Hangzhou, Zhejiang 310018, China, Tel. +86-571-8691-9158; email: 3204150144@qq.com (J.L. Qin)

Received 15 January 2020; Accepted 11 July 2020

ABSTRACT

The heterogeneous catalyst of CeO₂/ZSM5 was applied to hydrolyze Congo red in subcritical water for the first time in the present study. The hydrolysis rate of Congo red could be significantly accelerated by introducing only 5 mg of 5% CeO₂/ZSM5. The Congo red could be completely hydrolyzed at 220°C for 2 min—a reaction temperature 40°C lower than in the absence of 5% CeO₂/ZSM5. In addition, the 5% CeO₂/ZSM5 could be recycled for another run, and its Congo red hydrolysis efficiency and surface morphology showed no obvious change after 3 runs of recycling. The hydrolysis kinetics of Congo red in subcritical water could be well expressed by the Weibull model. The activation energy for hydrolysis of Congo red in subcritical water in the presence of 5% CeO₂/ZSM5 (104.8 kJ mol⁻¹) was much lower than in the absence of 5% CeO₂/ZSM5 (155.9 kJ mol⁻¹). The frequency factors were calculated to be 8.1×10^9 and 1.9×10^{14} min⁻¹ in the presence and absence of 5% CeO₂/ZSM5, respectively. With these excellent properties, 5% CeO₂/ZSM5 may prove to be an advantageous catalyst for the hydrolysis of Congo red in textile wastewater, in subcritical water.

Keywords: CeO₂/ZSM5; Congo red; Subcritical water; Hydrolysis kinetics; Regenerable; Weibull model

1. Introduction

Worldwide environmental problems caused by industrial water effluents, often containing color contamination, have received intensive concern because of their toxic, color and carcinogenic properties [1–5]. Azo dyes, which accounted for 70% of the dye produced every year, are the major dye residue in textile wastewater [6,7]. Significant efforts have been made to remove azo dye from textile wastewater, by physical, chemical oxidative and biological processes, such as the Fenton process, photocatalysis, solid-phase extraction and coagulation [3,8,9]. However,

these processes all have limitations. For example, the solid waste remaining after physical treatment is difficult to dispose of, while the biological treatment requires a long treatment time and has strong selectivity [3,10]. Therefore, new technologies are urgently needed, that can treat textile wastewater effectively and at a low cost.

Subcritical water treatment that employs only water as a reaction solvent has been proposed as an environmentally friendly technique for hydrolyzing potential pollutants. Compared with water at ambient temperature, such water has the unique properties of a lower relative dielectric

* Corresponding author.

constant and higher ion product. For example, when the water was heated to around 250°C under pressure conditions, its relative dielectric constant reduced from 80 to ~27, similar to those of methane and acetone at ambient temperature [11]. Meanwhile, the ion product of water increased to 10^{-11} , 1,000 times larger than water at ambient temperature. The low relative dielectric constant resulted in the high solubility of organic pollutants in subcritical water, which was a benefit for hydrolysis of organic pollutants; the high ion product makes subcritical water act as an acid and base catalyst to hydrolyze organic pollutants that could not be hydrolyzed by water at ambient temperature. Therefore, subcritical water is widely used to hydrolyze wastes, including compounds like biomass, aromatics, sludges and wastewater [3,11–14]. Donlagic and Levec [15] hydrolyzed Orange II at a reaction temperature range of 180°C–240°C at an oxygen partial pressure of 10–30 bar. They suggested that Orange II is decomposed, first thermally and oxidatively to aromatic intermediates, and then to carbon dioxide, via organic acids. Hosseini et al. [16] successfully decomposed and decolorized 4-(2-hydroxy naphthyl azo) benzenesulfonic acid sodium (AO7) in subcritical water, and found that the major decomposition products from AO7 were phenol, 2-naphthalenol and N-(phenyl methylene)benzenamine [16]. To improve the hydrolysis efficiency of an azo dye, oxidants and homogeneous catalysts such as H_2O_2 , Na_2CO_3 and $Cu(NO_3)_2$ have been introduced into subcritical water [3,17–19]. However, the utilization of oxidant and homogeneous metal catalysts can cause stainless steel reactors to corrode, and these catalysts are also hard to recycle. Heterogeneous metal catalysts, which could be recycled and reused after the reaction, could effectively overcome these drawbacks. Metal oxides of CeO_2 and MnO_2 are widely employed as catalysts for the degradation of organic pollutants such as methyl orange, reactive brilliant blue and cyclohexane, due to their excellent redox characteristics [20–22]. In addition, CeO_2 is the most naturally abundant and inexpensive rare earth element, and MnO_2 is a low-cost, abundant, and environmentally friendly material [20,23]. In our previous research, we found that the presence of copper ions in subcritical water could greatly accelerate the hydrolysis of Rhodamine B [3]. Therefore, heterogeneous metal catalysts (CeO_2 , MnO_2

and CuO) supported by ZSM5, a widely used catalyst supporter with intricate micropores and strong acidity, were synthesized via an impregnation method, in this study [24]. The hydrolysis behavior of Congo red, (serving as a model of azo dye) was investigated in subcritical water in the presence of a catalyst. Further, the hydrolysis kinetics of Congo red in subcritical water were also investigated.

2. Experimental setup

2.1. Materials

The reagents Congo red, copper nitrate hydrate, manganese acetate tetrahydrate, cerium nitrate hexahydrate and nano cerium oxide were provided by Aladdin Industrial Corporation (Shanghai, China). The chemical structure of Congo red is shown in Fig. 1.

2.2. Catalyst preparation and characterization

The catalysts ($CeO_2/ZMS5$, $MnO_2/ZMS5$ and $CuO/ZMS5$) were synthesized with the impregnation method. First, 0.127 g of cerium nitrate hexahydrate was dissolved in 1.4 mL of deionized water and then 1 g of ZSM5 was introduced into the solution. Subsequently, the sample was aged at room temperature for 12 h. After aging, the sample was dried at 100 °C and the dried sample was calcined at 500°C for 4 h. The prepared sample was designated as 5% $CeO_2/ZMS5$. The catalysts of 10% $CeO_2/ZMS5$, 15% $CeO_2/ZMS5$, 5% $MnO_2/ZMS5$, 10% $MnO_2/ZMS5$, 15% $MnO_2/ZMS5$, 5% $CuO/ZMS5$, 10% $CuO/ZMS5$ and 15% $CuO/ZMS5$ were prepared by the same method using an appropriate amount of metal salts solution. X-ray diffraction (XRD) patterns of prepared catalysts were obtained with a Rigaku Ultima IV diffractometer using monochromated $Cu K\alpha$ radiation. The surface morphology and elementary distribution were analyzed by an FEI Apreo Hivac scanning electron microscopy equipped with energy-dispersive X-ray spectroscopy (EDX).

2.3. Hydrolysis of Congo red in subcritical water

The hydrolysis of Congo red in subcritical water was carried out using a batch reactor as described in our previous research [3]. A volume of 7 mL of Congo red (125 mg L^{-1}),

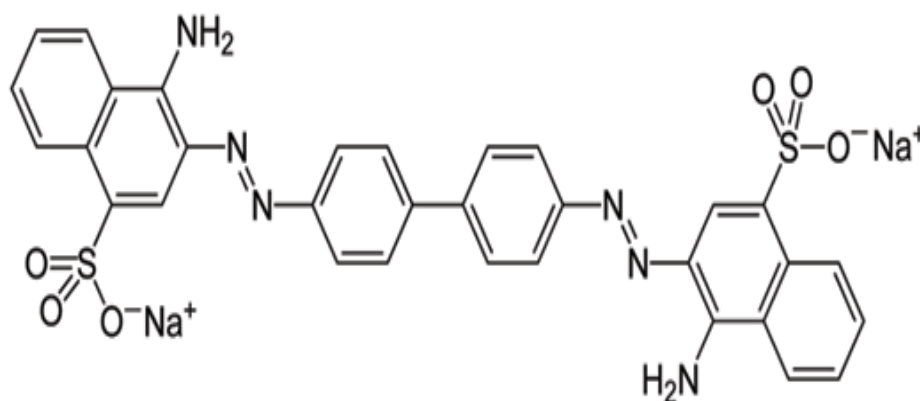


Fig. 1. Chemical structure of Congo red.

either with (5, 10 or 20 mg) or without catalyst was charged into the reactor. The reactor was then tightly closed and placed into a ceramics furnace that was preheated to 500°C. The reactor was treated at a reaction temperature range from 140°C to 260°C with reaction times of 2, 4, 6, 8 and 10 min. After the reaction time had elapsed, the reactor was cooled in an ice bath to stop the reaction. The reaction mixture was centrifuged and the recycled catalyst was dried at 105°C for 24 h. The concentration of Congo red in the centrifuged reaction mixture was measured by a CP visible spectrophotometer (Shanghai Spectrum, Shanghai China) at 497 nm with water as a blank. Each centrifuged reaction mixture was measured in triplicate.

3. Results and discussion

3.1. XRD patterns of catalysts

Fig. 2 shows the XRD patterns of CeO₂/ZMS5, CuO/ZMS5 and MnO₂/ZMS5. It can be observed that ZMS5 showed intense specific peaks in the range of 2θ = 22°–25° for all the catalysts. The diffraction peaks at 2θ = 28.5°, 33.1°, 47.6° and 56.4° attributed to CeO₂ could be clearly observed in CeO₂/ZMS5. These peaks increased intensely with CeO₂ content while the peaks corresponding to ZMS5 decreased. Diffraction peaks assigned to CuO (2θ = 35.5° and 38.7°) and MnO₂ (2θ = 30.1°, 45.5° and 55.4°) could be also observed in CuO/ZMS5 and MnO₂/ZMS5, respectively. In addition, the EDX analysis shown in Fig. 3 also confirmed the presence of Ce, Cu and Mn over the 10% CeO₂/ZMS5, 10% CuO/ZMS5 and 10% MnO₂/ZMS5 surfaces, respectively. The above results indicated that metal oxides were successfully supported over ZMS5 through the impregnation method.

3.2. Hydrolysis of Congo red in subcritical water in the presence of various catalysts

Fig. 4 shows the fraction of the remaining Congo red in the reaction mixture treated at 220°C for 2 min in the

presence of various catalysts. It can be observed that the hydrolysis of Congo red was promoted by the addition of catalysts into subcritical water. The catalyst of CeO₂/ZMS5 showed the highest Congo red hydrolysis ability among all the catalysts, whereas the nano CeO₂ had the lowest Congo red hydrolysis ability. The order of Congo red hydrolysis ability was CeO₂/ZMS5 > CuO/ZMS5 > MnO₂/ZMS5 > nano CeO₂ > non-catalyst. The hydrolysis ability of ZMS5 could not be determined, due to the formation of intermediates. Fig. 5 shows the effect of metal oxide loading value on the hydrolysis of Congo red at 220°C for 2 min. We could observe that the loading value of CeO₂ had no effect on the hydrolysis of Congo red, while 100% of Congo red was hydrolyzed even at the CeO₂ loading value of 5%. In contrast, the CuO/ZMS5 and MnO₂/ZMS5 showed lower Congo red hydrolysis efficiencies compared with that of CeO₂/ZMS5 at the same metal oxide loading value. The Congo red hydrolysis efficiencies of CuO/ZMS5 and MnO₂/ZMS5 increased with increasing metal oxide loading value and reached 95.6% and 86.8%, respectively, at the metal oxide

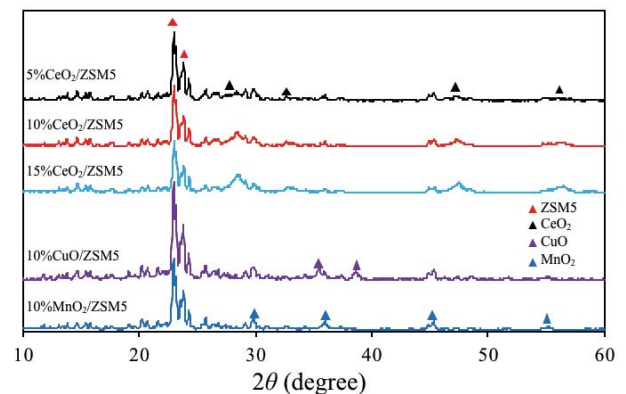


Fig. 2. XRD patterns of CeO₂/ZMS5, CuO/ZMS5 and MnO₂/ZMS5.

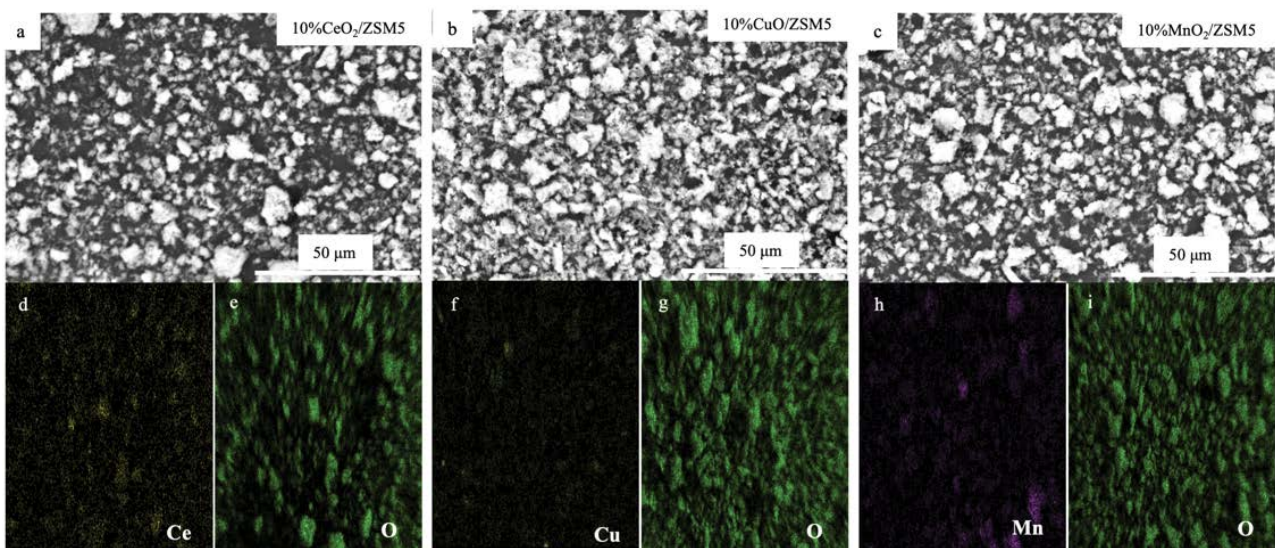


Fig. 3. EDX mapping of 10% CeO₂/ZMS5, 10% CuO/ZMS5 and 10% MnO₂/ZMS5.

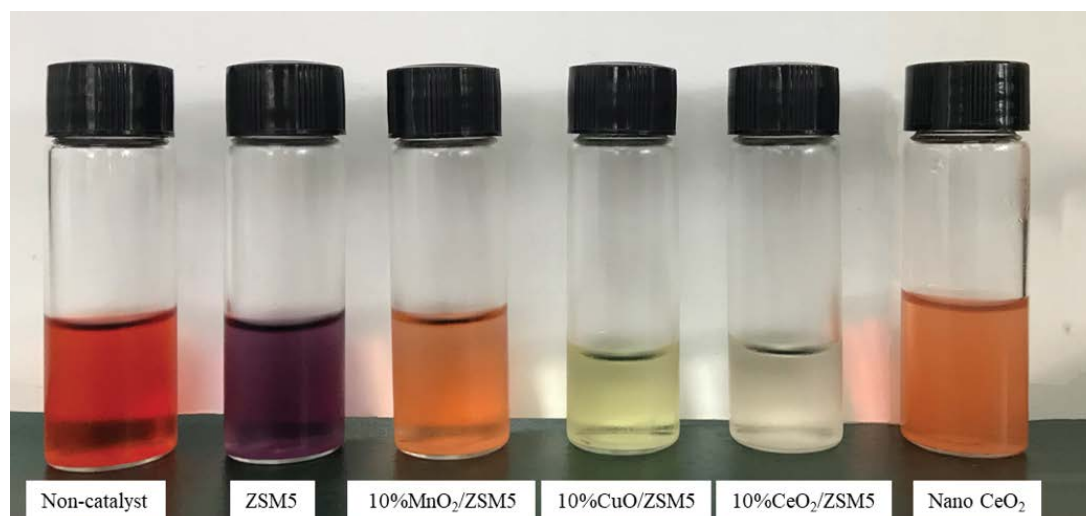


Fig. 4. Effect of catalyst on the hydrolysis of Congo red at the reaction temperature of 220°C for 2 min.

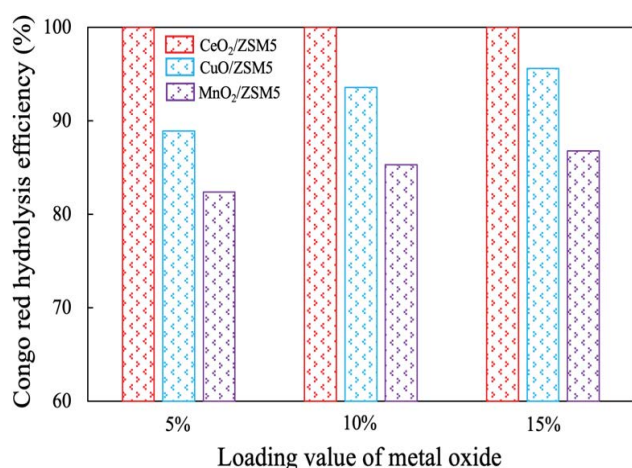


Fig. 5. Effect of metal oxide loading value over ZSM5 on the hydrolysis of Congo red at 220°C for 2 min.

loading value of 15%. The above results indicated that CeO₂/ZSM5 was an excellent catalyst for hydrolyzing Congo red in subcritical water. Catalyst dosage is an important factor that affects the cost of treatment of textile wastewater, in addition to metal oxide loading value. We therefore further evaluated the effect of CeO₂/ZSM5 dosage on the hydrolysis of Congo red in subcritical water. We found that the CeO₂/ZSM5 dosage had a negligible effect on the hydrolysis of Congo red in subcritical water (data not shown) and that Congo red could be efficiently hydrolyzed by using only 5 mg of 5% CeO₂/ZSM5. Therefore, 5% of CeO₂/ZSM5 was selected to hydrolyze Congo red in subcritical water.

3.3. Effects of reaction temperature and reaction time on hydrolysis of Congo red in subcritical water

Fig. 6 shows the effects of reaction temperature and reaction time on the hydrolysis of Congo red in subcritical water. The Congo red could indeed be efficiently

hydrolyzed in subcritical water. The Congo red remaining in the reaction mixture decreased with increasing reaction temperature, and it was completely hydrolyzed at 260°C (Fig. 6a). Meanwhile, the color of the reaction mixture became lighter at higher reaction temperatures, becoming colorless at the reaction temperature of 260°C. The hydrolysis rate of Congo red was greatly elevated when 5 mg of 5% CeO₂/ZSM5 was introduced into the subcritical water. The reaction temperature for complete hydrolysis of Congo red dropped to 220°C–40°C lower than that in the absence of 5% CeO₂/ZSM5. The hydrolysis of Congo red was accelerated with long reaction time, and the reaction time for complete hydrolysis of Congo red became shorter at higher reaction temperatures (Figs. 6b and c). The spent 5% CeO₂/ZSM5 could be used for the next run to hydrolyze Congo red at 200°C, and the hydrolysis efficiency showed no obvious change after 3 runs of recycling (Fig. 7). In addition, the surface morphology of 5% CeO₂/ZSM5 after 3 runs of recycling showed no obvious change compared with that of raw 5% CeO₂/ZSM5, indicating a high stability of the catalyst (Fig. 8). The reusability of 5% CeO₂/ZSM5, together with the higher Congo red hydrolysis efficiency, lower catalyst dosage and metal oxide loading value, compared to those of 5% CuO/ZSM5 and 5% MnO₂/ZSM5, makes this a promising catalyst for the hydrolysis of Congo red in subcritical water.

3.4. Hydrolysis kinetics of Congo red in subcritical water

The Weibull model, a very flexible model for expressing different types of reaction, was applied to describe the hydrolysis kinetics of Congo red in subcritical water [3,25]. The description of the Weibull equation is as follows:

$$\frac{C}{C_0} = \exp\left[-(kt)^n\right] \quad (1)$$

where k , t and n are the rate constant (min⁻¹), shape constant and reaction time (min), respectively. Eq. (1) could be further converted to:

$$\ln \left[-\ln \left(\frac{C}{C_0} \right) \right] = n(\ln t + \ln k) \quad (2)$$

A plot of $\ln[-\ln(C/C_0)]$ vs. $\ln t$ generated a straight line, the slope and intercept of which could be employed to calculate the rate and shape constants, respectively. As shown in Fig. 9, the Weibull equation showed high conformity with the experimental data ($r^2 > 0.93$), indicating that the hydrolysis kinetics of Congo red in subcritical water could be well expressed by the Weibull equation. The rate constants for hydrolysis of Congo red in subcritical water were 0.002, 0.04, 0.25, 0.48 and 1.03 min^{-1} at the reaction temperatures of 140°C, 160°C, 180°C, 200°C and 220°C, respectively. The rate constant at each reaction temperature became larger when

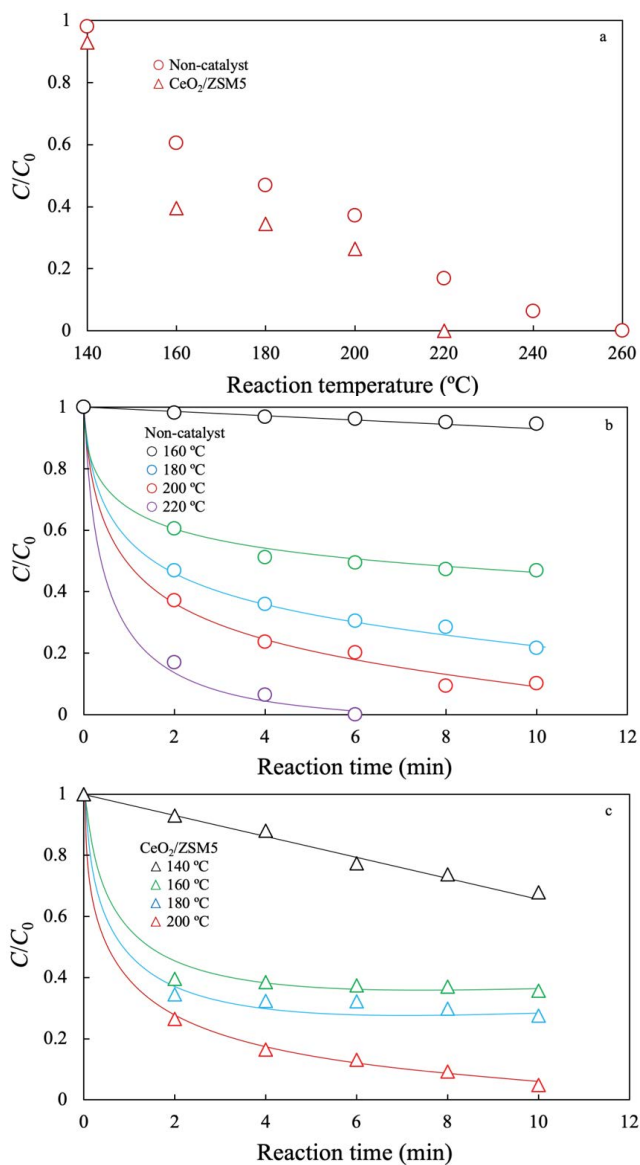


Fig. 6. Effect of (a) reaction temperature and reaction time on the hydrolysis of Congo red in subcritical water in the (b) absence and (c) presence of 5% $\text{CeO}_2/\text{ZSM5}$.

5% $\text{CeO}_2/\text{ZSM5}$ was added into the subcritical water, and its values were 0.042, 0.13, 0.8 and 0.86 min^{-1} at the reaction temperatures of 140°C, 160°C, 180°C and 200°C, respectively. The above rate constants were much larger than those obtained from photocatalytic degradation of Congo red by $\text{Co}_3\text{O}_4/\text{TiO}_2/\text{Graphene oxide}$, Ag/ZnO or Pd/ZnO [26,27], indicating the high hydrolysis efficiency of 5% $\text{CeO}_2/\text{ZSM5}$ in subcritical water. The shape constant obtained from hydrolysis of Congo red by subcritical water in the presence of 5% $\text{CeO}_2/\text{ZSM5}$ was much lower than that in the absence of 5% $\text{CeO}_2/\text{ZSM5}$, indicating its higher Congo red hydrolysis rate.

Based on the rate constant and Arrhenius equation, the activation energy and frequency factor could be calculated. The Arrhenius equation could be written as follows:

$$k = A \exp \left(-\frac{E}{RT} \right) \quad (3)$$

where A , E , R and T are the frequency factor (min^{-1}), activation energy (kJ mol^{-1}), universal gas constant ($\text{kJ mol}^{-1} \text{K}^{-1}$) and absolute temperature (K), respectively. As shown in Fig. 10, the plotted $\ln k$ vs. $1/T$ showed straight lines for the hydrolysis of Congo red in subcritical water in the presence and absence of 5% $\text{CeO}_2/\text{ZSM5}$, with correlation values of 0.93 and 0.92, respectively. The calculated activation energies were 104.8 and 155.9 kJ mol^{-1} for hydrolysis of Congo red in subcritical water in the presence and absence of 5% $\text{CeO}_2/\text{ZSM5}$, respectively. The above activation energies were much higher than those obtained from the degradation of Congo red by Fenton reaction in the presence of $\text{Fe}_3\text{O}_4/\text{ZnO}$ (19.01 kJ mol^{-1}) or $\text{Fe}_3\text{O}_4/\text{ZnO}/\text{Graphene}$ (18.64 kJ mol^{-1}) catalyst [28], because of the difference in the reaction mechanism. The frequency factors for hydrolysis of Congo red in the presence and absence of 5% $\text{CeO}_2/\text{ZSM5}$ were calculated to be 8.1×10^9 and $1.9 \times 10^{14} \text{min}^{-1}$, respectively.

To investigate the synergistic effect between ZSM5 and CeO_2 , the Congo red hydrolysis ability of CeO_2 and ZSM5 mixture was evaluated at 200°C. The color of reaction mixtures obtained from the hydrolysis of Congo red in the presence of ZSM5 (purple) and nano CeO_2 (orange)

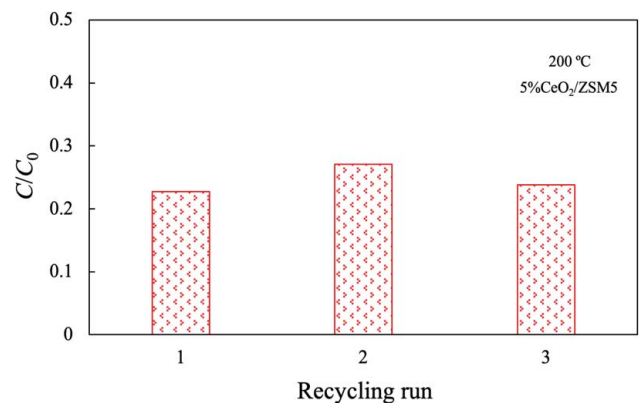


Fig. 7. Congo red hydrolysis efficiency of 5% $\text{CeO}_2/\text{ZSM5}$ after 3 runs of recycling.

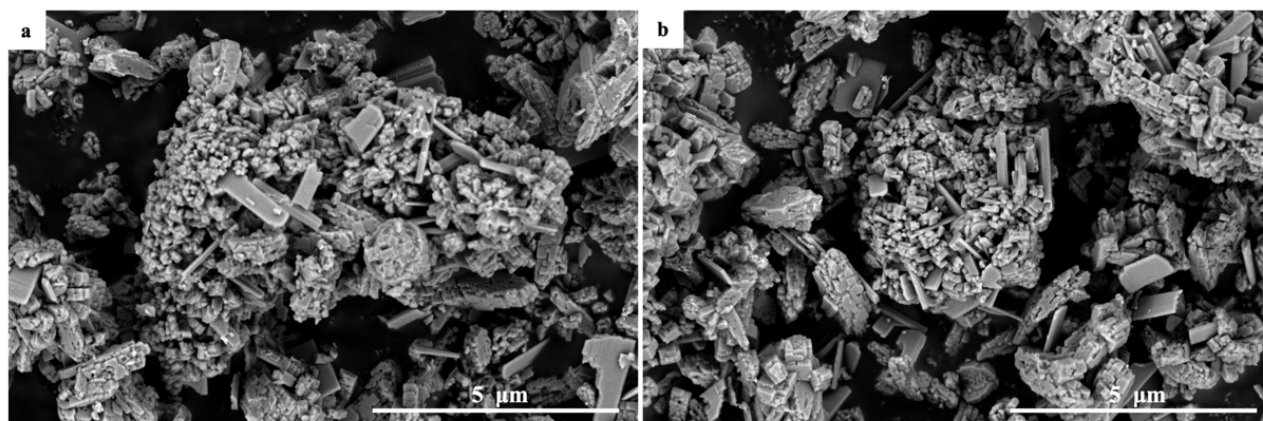


Fig. 8. Surface morphologies of 5% CeO₂/ZSM5 (a) before and (b) after 3 runs of recycling.

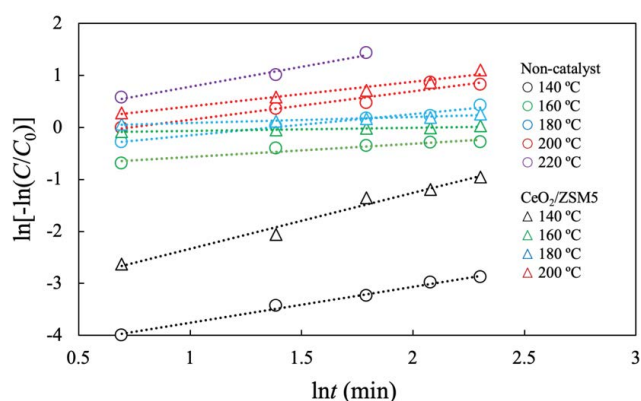


Fig. 9. Application of Weibull model to hydrolysis of Congo red at 140°C, 160°C, 180°C, 200°C and 220°C in the absence of 5% CeO₂/ZSM5 and 140°C, 160°C, 180°C and 200°C in the presence of 5% CeO₂/ZSM5.

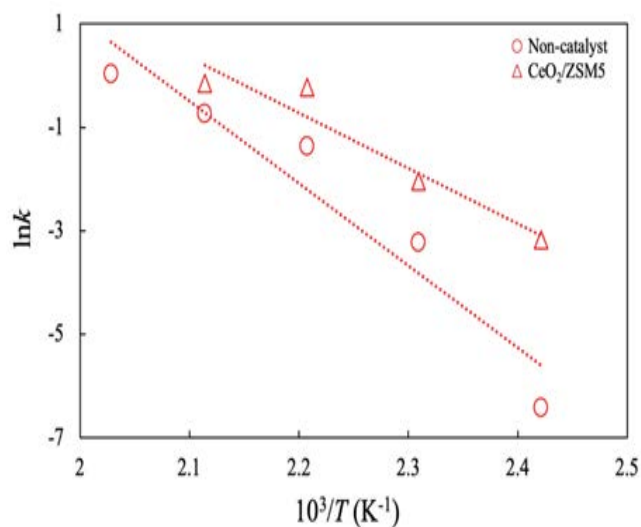


Fig. 10. Arrhenius plot for the hydrolysis of Congo red in subcritical water in the absence and presence of 5% CeO₂/ZSM5.

was similar to those shown in Fig. 4. However, the color of reaction mixtures obtained from hydrolysis of Congo red in the presence of ZSM5 and a nano CeO₂ mixture became light purple compared with that in the presence of ZSM5, probably because the Congo red could be continuously hydrolyzed by nano CeO₂ on a base of ZSM5, resulting in the lighter color of the reaction mixture, compared with that of ZSM5 alone. The reaction mixture became colorless during the hydrolysis of Congo red in the presence of 5% CeO₂/ZSM5, indicating that a stronger synergistic effect between ZSM5 and CeO₂ was formed in 5% CeO₂/ZSM5. The detailed mechanism of CeO₂/ZSM5 for hydrolysis of Congo red in subcritical water will be investigated in our future research.

4. Conclusions

The hydrolysis of Congo red, which served as a model of azo dye in textile wastewater, was conducted in subcritical water, in the presence of CeO₂/ZSM5 catalyst. The Congo red could be efficiently hydrolyzed at 220°C in a reaction time of 2 min by adding only 5 mg of 5% CeO₂/ZSM5, and the reaction temperature was 40°C lower than that in the absence of 5% CeO₂/ZSM5. The 5% CeO₂/ZSM5 also showed high recycling ability, as the Congo red hydrolysis efficiency showed no obvious change after 3 runs of recycling. The Weibull model was employed to express the hydrolysis kinetics of Congo red in subcritical water. The activation energies and frequency factors for hydrolysis of Congo red in subcritical water in the presence and absence of 5% CeO₂/ZSM5 were calculated to be 104.8 and 155.9 kJ mol⁻¹, and 8.1 × 10⁹ and 1.9 × 10¹⁴ min⁻¹, respectively. Therefore, it was considered that 5% CeO₂/ZSM5 is an excellent catalyst for the hydrolysis of Congo red in subcritical water.

Acknowledgments

This work was financially supported by the Zhejiang Basic Public Welfare Research Project (Grant No. LGG18E080006) and the Huzhou Science and Technology Project (Grant No. 2018ZD2026). A portion of this work was supported by the Research Project of Zhejiang Provincial Department of Education (Grant No. Y201839475).

References

- [1] N.K. Amin, Removal of direct blue-106 dye from aqueous solution using new activated carbons developed from pomegranate peel: adsorption equilibrium and kinetics, *J. Hazard. Mater.*, 165 (2009) 52–62.
- [2] M. Styliadi, D.I. Kondarides, X.E. Verykios, Pathways of solar light-induced photocatalytic degradation of azo dyes in aqueous TiO₂ suspensions, *Appl. Catal., B*, 40 (2003) 271–286.
- [3] K. Cheng, W. Yang, H. Wang, J. Zhou, S.J. Wu, T.M. Yu, J.B. Pan, Effect of Cu(II) on degradation and decolorization of rhodamine B in subcritical water, *Chem. Res. Chin. Univ.*, 33 (2017) 643–647.
- [4] Z.X. Fang, Y. Chen, B.R. Wang, S.H. Jiao, G.S. Pang, Heterostructure Ag@WO_{3-x} composites with high selectivity for breaking azo-bond, *Chem. Res. Chin. Univ.*, 34 (2018) 517–522.
- [5] Q.B. Si, Q. Wen, Q.B. Yang, Y. Song, Y.X. Li, Preparation of β -cyclodextrin/Fe₃O₄/polyvinylpyrrolidone composite magnetic microspheres for the adsorption of methyl orange, *Chem. Res. Chin. Univ.*, 33 (2017) 1012–1016.
- [6] Y. Pan, T. Zhu, Z. He, Enhanced removal of azo dye by a bioelectrochemical system integrated with a membrane biofilm reactor, *Ind. Eng. Chem. Res.*, 57 (2018) 16433–16441.
- [7] D. Rawat, V. Mishra, R.S. Sharma, Detoxification of azo dyes in the context of environmental processes, *Chemosphere*, 155 (2016) 591–605.
- [8] S.-F. Yang, C.-G. Niu, D.-W. Huang, H. Zhang, C. Liang, G.-M. Zeng, SrTiO₃ nanocubes decorated with Ag/AgCl nanoparticles as photocatalysts with enhanced visible-light photocatalytic activity towards the degradation of dyes, phenol and bisphenol A, *Environ. Sci. Nano*, 4 (2017) 485–595.
- [9] A.A. Bhatti, M. Oguz, M. Yilmaz, Magnetizing calixarene: azo dye removal from aqueous media by Fe₃O₄ nanoparticles fabricated with carboxylic-substituted calix[4]arene, *J. Chem. Eng. Data*, 62 (2017) 2819–2825.
- [10] Y. Zhang, F. Gao, B. Wanjala, Z.Y. Li, G. Cernigliaro, Z.Y. Gu, High efficiency reductive degradation of a wide range of azo dyes by SiO₂-Co core-shell nanoparticles, *Appl. Catal., B*, 199 (2016) 504–513.
- [11] W. Yang, T. Shimanouchi, S.J. Wu, Y. Kimura, Investigation of the degradation kinetic parameters and structure changes of microcrystalline cellulose in subcritical water, *Energy Fuels*, 28 (2014) 6974–6980.
- [12] W. Yang, H. Wang, J. Zhou, S.J. Wu, Hydrolysis kinetics and mechanism of chitin in subcritical water, *J. Supercrit. Fluids*, 135 (2018) 254–262.
- [13] I.M. Svishchev, A. Plugatyr, Supercritical water oxidation of *o*-dichlorobenzene: degradation studies and simulation insights, *J. Supercrit. Fluids*, 37 (2006) 94–101.
- [14] N. Kazemi, O. Tavakoli, S. Seif, M. Nahangi, High-strength distillery wastewater treatment using catalytic sub- and supercritical water, *J. Supercrit. Fluids*, 97 (2015) 74–80.
- [15] J. Donlagić, J. Levec, Comparison of catalyzed and non-catalyzed oxidation of azo dye and effect on biodegradability, *Environ. Sci. Technol.*, 32 (1998) 1294–1302.
- [16] S.D. Hosseini, F.S. Asghari, H. Yoshida, Decomposition and decoloration of synthetic dyes using hot/liquid (subcritical) water, *Water Res.*, 44 (2010) 1900–1908.
- [17] V.M. Daskalaki, E.S. Timotheatou, A. Katsaounis, D. Kalderis, Degradation of Reactive Red 120 using hydrogen peroxide in subcritical water, *Desalination*, 274 (2011) 200–205.
- [18] A. Yuksel, M. Sasaki, M. Goto, Complete degradation of Orange G by electrolysis in sub-critical water, *J. Hazard. Mater.*, 190 (2011) 1058–1062.
- [19] B. Kayan, B. Gözmen, Degradation of Acid Red 274 using H₂O₂ in subcritical water: application of response surface methodology, *J. Hazard. Mater.*, 201–202 (2012) 100–106.
- [20] N. Zhang, G.M. Zhang, S. Chong, H. Zhao, T. Huang, J. Zhu, Ultrasonic impregnation of MnO₂/CeO₂ and its application in catalytic sono-degradation of methyl orange, *J. Environ. Manage.*, 205 (2018) 134–141.
- [21] C.Y. Su, W.G. Li, X.Z. Liu, X.F. Huang, X.D. Yu, Fe-Mn-sepiolite as an effective heterogeneous Fenton-like catalyst for the decolorization of reactive brilliant blue, *Front. Environ. Sci. Eng.*, 10 (2016) 37–45.
- [22] S.S. Lin, C.L. Chen, D.J. Chang, C.C. Chen, Catalytic wet air oxidation of phenol by various CeO₂ catalysts, *Water Res.*, 36 (2002) 3009–3014.
- [23] H.H. Zhang, J.N. Gu, J. Tong, Y.F. Hu, B. Guan, B. Hu, J. Zhao, C.Y. Wang, Hierarchical porous MnO₂/CeO₂ with high performance for supercapacitor electrodes, *Chem. Eng. J.*, 286 (2016) 139–149.
- [24] F.J. Liu, T. Willhammar, L. Wang, L.F. Zhu, Q. Sun, X.J. Meng, W. Carrillo-Cabrera, X.D. Zou, F.-S. Xiao, ZSM-5 zeolite single crystals with *b*-axis-aligned mesoporous channels as an efficient catalyst for conversion of bulky organic molecules, *J. Am. Chem. Soc.*, 134 (2012) 4557–4560.
- [25] S.H. Khajavi, Y. Kimura, T. Omori, R. Matsuno, S. Adachi, Degradation kinetics of monosaccharides in subcritical water, *J. Food Eng.*, 68 (2005) 309–313.
- [26] W.-K. Jo, S. Kumar, M.A. Isaacs, A.F. Lee, S. Karthikeyan, Cobalt promoted TiO₂/GO for the photocatalytic degradation of oxytetracycline and Congo red, *Appl. Catal., B*, 201 (2017) 159–168.
- [27] N. Güy, M. Özacar, The influence of noble metals on photocatalytic activity of ZnO for Congo red degradation, *Int. J. Hydrogen Energy*, 41 (2016) 20100–20112.
- [28] R. Saleh, A. Taufik, Degradation of methylene blue and congo-red dyes using Fenton, photo-Fenton, sono-Fenton, and sonophoto-Fenton methods in the presence of iron(II,III) oxide/zinc oxide/graphene (Fe₃O₄/ZnO/graphene) composites, *Sep. Purif. Technol.*, 210 (2019) 563–573.